Article

Studies of Polylactic Acid and Metal Oxide Nanoparticles-Based Composites for Multifunctional Textile Prints

Meram S. Abdelrahman [1], Sahar H. Nassar [1], Hamada Mashaly [1], Safia Mahmoud [1], Dalia Maamoun [2], Mohamed El-Sakhawy [3],*⬦, Tawfik A. Khattab [1]⬦ and Samir Kamel [3]

[1] Dyeing, Printing and Auxiliaries Department, Textile Industries Research Division, National Research Centre, Cairo 12622, Egypt; ms.abdel-rahman@nrc.sci.eg (M.S.A.); sh.wahab@nrc.sci.eg (S.H.N.); hamada_mashaly@yahoo.com (H.M.); sofyalie@yahoo.com (S.M.); tkhattab@kent.edu (T.A.K.)

[2] Printing/Dyeing/Finishing Department, Faculty of Applied Arts, Helwan University, Cairo 11795, Egypt; daliamaamoun@gmail.com

[3] Cellulose and Paper Department, National Research Centre, Cairo 12622, Egypt; samirki@yahoo.com

* Correspondence: elsakhawy@yahoo.com

check for updates

Abstract: A novel approach toward the production of multifunctional printed technical textiles is reported. Three different metal oxides nanoparticles including titanium dioxide, magnesium oxide, and zinc oxide were prepared and characterized. Both natural wool and synthetic acrylic fibers were pretreated with the prepared metal oxide nanoparticles followed by printing using polylactic acid based paste containing acid or basic dyestuffs. Another route was applied via post-treatment of the targeted fabrics with the metal oxide nanoparticles after running the printing process. The color strength (*K/S*) and colorfastness properties of pretreated and post-treated printed fabrics were evaluated and compared with untreated printed fabrics. The presence of nanoparticles on a fabric surface during the coating process was found to significantly increase the color strength value of the coated textile substrates. The increased *K/S* value depended mainly on the nature and concentration of the applied metal oxide, as well as the nature of colorant and fabric. In addition, the applied metal oxide nanoparticles imparted the printed fabrics with good antibacterial activity, high ultraviolet protection, photocatalytic self-cleaning, and improved colorfastness properties. Those results suggest that the applied metal oxide-based nanoparticles could introduce ideal multifunctional prints for garments.

Keywords: polylactic acid; metal oxide nanoparticles; UV protection; self-cleaning; antibacterial

1. Introduction

Technical textiles are high-performance smart materials designed not just to appear good-looking, but also to introduce a considerable added functional value toward a better quality of life [1–3]. Technical textiles have been applied in modern society for various specialized applications, such as antimicrobial, super hydrophobic, anti-static, ultraviolet protection, flame-retardant and self-cleaning purposes [4–8]. Nanotechnology can be considered as one of the most significant emerging global technologies. It is a creative technique for a lot of industrial sectors [9–11]. Recognized advantages of employing nanotechnology and nanomaterials in textile industry can be debated in terms of the high surface area per unit weight leading to better material activity, lower usage of chemicals, less energy consumption and cost, and less ecological impacts as well as lower effects on the fabric's inherent physical and mechanical characteristics, such as handle, strength and air-permeability [12–19]. In the past few years, numerous research and industrial attempts have been assigned toward the development of novel innovative goods toward a better human life [20–23]. Textile production, as

one of the most pertinent and ever-progressive manufacturing fields all over the globe, is not an exception. In particular, with an increasing knowledge in individual healthcare and hygiene, garments with antibacterial performance are becoming an attractive ground for both textiles producers and researchers [24,25]. Humans are usually infected by microbes such as bacteria, mold, yeast and viruses. Recently, antimicrobial active materials have been utilized in industry, such as quaternary ammonium. Regrettably, such agents are either poisonous or weakly efficient making them inappropriate for application in various industrial fields, such as foodstuffs, filters and garments [26–31]. In contrast, metal oxide-based nanoparticles are not toxic and disinfectants that can considerably decrease many microbial infections. Metal oxides-based nanoparticles usually show excellent physicochemical properties due to their higher surface-to-volume ratio. Titanium dioxide (TiO_2), magnesium oxide (MgO) and zinc oxide (ZnO) nanoparticles are interesting materials due to their multifunctional properties and cheapness [32–35].

Different approaches have been explored for the incorporation of metal oxide nanoparticles onto both natural and synthetic textile fibers, such as sol-gel, sonochemical printing, pad-batch, dip-coating and exhaustion procedures [36–39]. The exhaustion process can be defined as the adsorption of a certain material onto the fabric which is impregnated in a material aqueous bath. Thus, the material concentration in the aqueous bath progressively decreases. The exhaustion rate can then be explored as a function of time. The exhaustion approach has been considered as the best method with the ability to introduce homogeneous distribution of metal oxide nanoparticles. Additionally, the exhaustion approach has been particularly suitable for concurrent deposition of nanoparticles and dyestuff onto fabric to establish dyed and antimicrobial garments as a one-step efficient process [40–43]. Several studies have been reported on the deposition of metal oxide nanoparticles onto dyed fabrics using the exhaustion method during the dyeing process. However, only few reports were described on the incorporation of metal oxide nanoparticles onto textiles during the printing process. Herein, we report for the first time, to the best of our knowledge, the application of metal oxide nanoparticles during the printing process using a polylactic acid-based synthetic thickener. In this study, we examined the incorporation of the metal oxide-based nanoparticles before and after running the screen-printing process using polylactic acid based paste. Metal oxides based nanoparticles titanium dioxide, magnesium oxide and zinc oxide were prepared to be applied on acrylic and wool fabrics using environmentally friendly polylactic based synthetic biodegradable thickener. Such treatment was employed to establish prints able to afford highly active surface that combines photocatalytic self-cleaning, antimicrobial activity and ultraviolet (UV) protection properties. Color strength and colorfastness properties were also evaluated.

2. Experimental Details

2.1. Materials and Substrates

Scoured wool (140 g/m^2) and acrylic (110 g/m^2) fabrics were provided from El Shorpagy Co., Cairo, Egypt. Colorants were kindly supplied from DyStar, Cairo, Egypt, including C.I. Basic Yellow 28 and C.I. Acid Red 88 (Figure 1). All materials and solvents were obtained from Fluka and Aldrich and were used without further purification. All experimental data were gathered at ambient conditions unless stated otherwise.
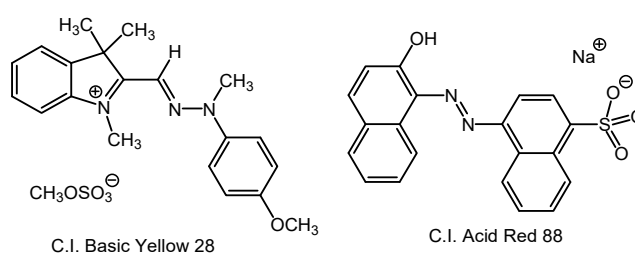
Figure 1. Molecular structure of the printed dyestuffs.

2.2. Preparation of Thickening Agents

The triglyceride polylactic acid (TGPLA) synthetic thickener was synthesized via thermal condensation of glycerin and lactic acid. A mixture of lactic acid and glycerol at a molar ratio of 98:2 together with 2–3 drops of sulfuric acid was mechanically stirred at 105 °C for 20 min. An aqueous solution of sodium hydroxide (1 M) was added slowly to the mixture followed by adding ethanol (100 mL) to give a wet gel-like precipitate that was filtered off under vacuum and air-dried conditions to afford a TGPLA thickening agent. On the other hand, the carboxy lactic methacrylate (CLMA) thickening agent was synthesized in *one-pot* reaction procedure by stirring a mixture of methacrylic acid (2%), lactic acid (98%) and few drops of sulfuric acid at 105 °C for 30 min. *N,N*-methylene diacrylamide (2 g) was then added to the reaction mixture followed by adding potassium persulfate (270 mg) and stirring for 10–15 min at 105 °C. Hydroquinone (110 mg) was then added to the mixture followed by cooling to room temperature. An aqueous solution of sodium hydroxide (1 M) was employed to neutralize the mixture. Ethanol (100 mL) was added to give a precipitate which was filtered off under vacuum and air-dried to give CLMA thickening agent as a white powder. The molecular structures of the prepared TGPLA and CLMA thickening agents are shown in Figure 2 [44,45].
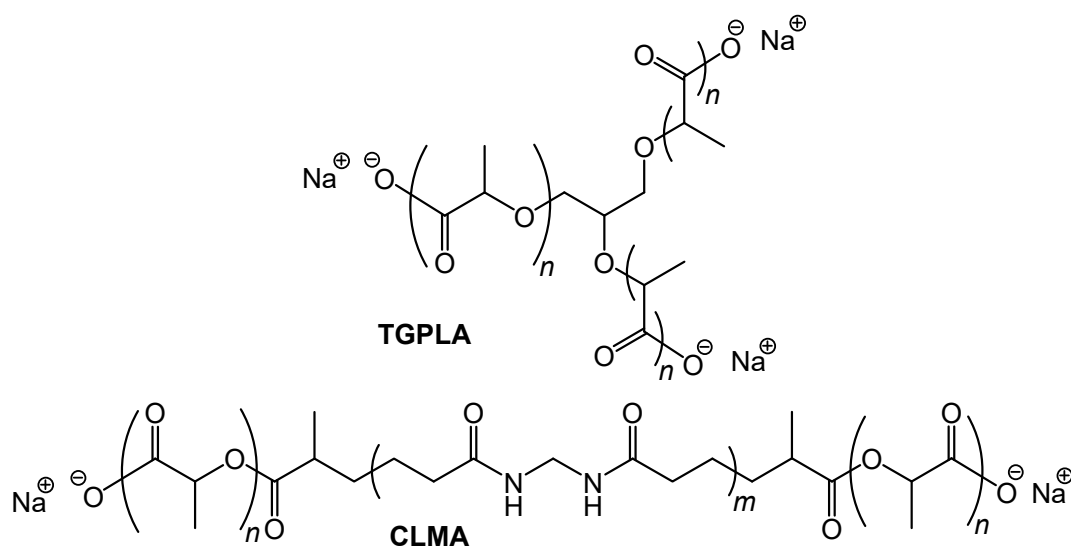
Figure 2. Chemical structures of triglyceride polylactic acid (TGPLA) and carboxy lactic methacrylate (CLMA) synthetic thickeners.

2.3. Preparation of Metal Oxide-Based Nanoparticles

2.3.1. Synthesis of ZnO Nanoparticles

Zinc oxide nanoparticles were prepared according to a procedure previously reported in the literature [46]. The preparation process was performed at a high level of super-saturation to accomplish a nucleation rate higher than growth rate. Zinc (II) chloride (5.5 g) was dissolved in distilled water (200 mL) at 90 °C using an oil bath. An aqueous solution of sodium hydroxide (16 mL of 5 M NaOH) was added slowly over 10 min at 90 °C to the previously prepared zinc chloride aqueous solution with a mild magnetic stirring. The produced particles were isolated from the supernatant solution by precipitation. The precipitate was washed with distilled water to reduce the total content of sodium chloride as a by-product. The full removal of sodium chloride was confirmed by an aqueous solution of silver nitrate. The particles were then gathered using *sec*-propanol and subjected to ultrasonic waves for 10 min under ambient conditions to disrupt the micro agglomerates leading to the liberation of ZnO nanoparticles. The produced nanoparticles were exposed to centrifugation at 6000 rpm for 20 min followed by thermal treatment at 250 °C for 5 h.

2.3.2. Synthesis of TiO$_2$ Nanoparticles

Titanium (IV) tetrachloride of 3.5 g was dispersed in 50 mL distilled water in an ice-bath followed by adding absolute ethanol (35 mL) with vigorous magnetic stirring for 30 min under ambient conditions. A few drops of NH$_3$·H$_2$O were added slowly and mixture was stirred vigorously. The solution was left to settle down overnight. The produced precipitate was subjected to centrifugation followed by washing with distilled water to remove chloride ion. The purified precipitate was then dried at 200 °C for 4 h to introduce amorphous TiO$_2$ which was calcinated at 400 °C for 4 h to give powder TiO$_2$ nanoparticles [46].

2.3.3. Synthesis of MgO nanoparticles

Magnesium oxide nanoparticles were prepared employing the sol-gel approach [46]. Magnesium chloride hexahydrate (100 g) was dissolved in distilled water (500 mL), to which an aqueous solution of sodium hydroxide (50 mL of 1N NaOH) was added. The mixture was vigorously magnetically stirred for 4 h to produce magnesium hydroxide [Mg(OH)$_2$] precipitate which was subjected to centrifugation at 3000 rpm for 5 min. The produced magnesium hydroxide gel was exposed to washing several times using distilled water and dried at 60 °C for 24 h and calcinated at 450 °C for 2 h to afford magnesium oxide nanoparticles.

2.4. Pre- and Post-Treatment of Wool and Acrylic Fabrics by Nanoparticles

Both wool and acrylic substrates were treated with ZnO, TiO$_2$ and MgO nanoparticles via exhaustion technique before (pre) and after (post) running the printing process. The fabrics were subjected to an impregnation process in an aqueous bath of ZnO, TiO$_2$ or MgO at four different concentration values (0.5%, 1.0%, 1.5%, and 2.0% owf; on-weight-fabric). The bath was then heated at 80 °C for 20 min. The applied liquor ratio was at 1:30 and the impregnation process was performed in presence of a dispersing agent to facilitate a homogenous suspension of the metal oxide nanoparticles in water. The fabrics were then subjected to padding and squeezed to 80% pick-up followed by drying at 60 °C. The padded samples treated with ZnO and TiO$_2$ nanoparticles were cured at 140 °C for 10 min, while the fabrics treated with MgO nanoparticles were cured at 120 °C for 3 min. Finally, the samples were exposed to washing at 60 °C for 20 min followed by air-drying.

2.5. Screen-Printing Technique

Both pre- and post-treated wool and acrylic fabrics were subjected to a screen-printed process using a printing paste prepared as shown in Tables 1 and 2.

Table 1. Printing paste for acid dyestuff.

Component	Weight (g)
Dye	30
Urea	50
Thioethylene glycol	50
Thickener	Y *
Water	X **
Ammonium sulphate	60
Ludigol	15
Total	1000

* The utilized synthetic thickening agent was either carboxy lactic methacrylate (CLMA) at 60 g/kg or triglyceride polylactic acid (TGPLA) at 80 g/kg. ** X is the weight of water used in the paste preparation upon completing the formula to 1000 g.

Table 2. Printing paste for basic dyestuff.

Component	Weight (g)
Dye	30
Acetic acid 30%	30
Thioethylene glycol	3
Thickener	Y *
Water	X **
Citric acid	5
Total	1000

* The utilized synthetic thickening agent was either carboxy lactic methacrylate (CLMA) at 60 g/kg or triglyceride polylactic acid (TGPLA) at 80 g/kg. ** X is the weight of water used in the paste preparation upon completing the formula to 1000 g.

The screen-printed fabrics were then exposed to a fixation process by steaming at 100–103 °C for 30 min. The fabrics dyed with an acid dye were then washed with tap water, soaped at 40–50 °C using 2 g/L nonionic detergent, washed with tap water, and finally air-dried at ambient conditions. The fabrics dyed with a basic dye were washed with tap water, soaped with 2 g/L nonionic detergent at 60 °C for 30 min, and finally air-dried at ambient conditions.

2.6. Analysis and Measurements

2.6.1. Morphology and Elemental Composition

Field-emission scanning electron microscopy (FE-SEM) was employed to study the morphological properties of the pre- and post-treated fabrics using Quanta FEG250 (Thermo Fisher Scientific, Brno, Czech Republic). This was equipped with energy-dispersive X-ray spectroscopy (TEAM-EDX Model) to study the chemical composition of the pre- and post-treated fabrics by applying a work distance at 21 mm and an acceleration voltage at 20 kV.

2.6.2. Color Strength and Colorfastness Properties

The color strength (*K/S*) of the screen-printed fabrics was investigated employing Hunter Lab UltraScanPro spectrophotometer. The screen-printed fabrics were exposed to the colorfastness studies, including washing, perspiration, rubbing and light depending on the standard procedures, ISO 105-CO4 (1989), ISO 105-EO4 (1989), ISO 105-X12 (1987) and ISO 105-BO2 (1988), respectively [47,48].

2.6.3. Antimicrobial Activity

The standard Kirby–Bauer disc agar diffusion approach was applied to measure the antimicrobial activity of both pre- and post-treated wool and acrylic fabrics against *Escherichia coli* (G−) and *Staphylococcus aurous* (G+). The disc agar diffusion method is a documented standard approach to measure the inhibition zone of a targeted sample [49].

2.6.4. Self-Cleaning Activity

The photocatalytic performance of both pre- and post-treated wool and acrylic fabrics was assessed by determining the decomposition progress of methylene blue (Aldrich, United States). The ultraviolet transmission through fabrics was assessed using a Cary Varian 300 ultraviolet-visible (UV-Vis) spectrophotometer in the wavelength range 320–400 nm. The photocatalytic self-cleaning performance was reported by monitoring the degradation of methylene blue under visible light at wavelengths higher than 410 nm. The visible light irradiation was afforded using a fluorescent lamp (TC-L18W, AC230V-50 Hz, China) at a distance of 5 cm and light intensity of 44 µW cm^{-2}). A wool/acrylic sample 1 g in 50 mL of an aqueous solution of methylene blue (10 mg/L at pH 6.5) was stirred for 30 min to accomplish an adsorption/desorption equilibrium among the photocatalysis and methylene blue under ambient conditions. The sample was then exposed to irradiation under visible

light. Following each irradiation interval time, about 5 mL of solution was taken and analyzed by spectrophotometer. The concentration of methylene blue was recorded by measuring the absorption maxima at 665 nm as a function of the irradiation time. The photocatalytic degradation was recorded using the following equation:

$$\text{Photocatalytic degradation} = (C_0 - C_t/C_0) = (A_0 - A_t/A_0)$$

where C_0 is the original concentration of methylene blue, C_t is the concentration at different irradiation time periods, A_0 is the initial absorption and A_t is the variable absorption at different irradiation time periods [50].

2.6.5. Ultraviolet Protection

The ultraviolet protection factor (UPF) was determined according to AS/NZS 4399:1996 standard procedure. The ultraviolet transmission through the fabric was determined by a Cary Varian 300 UV-Vis spectrophotometer under AATCC 183:2010 UVA Transmittance [51,52].

3. Results and Discussion

3.1. Preparation of Multifunctional Fabrics

The major aim of the current work was to study the multifunctional effects imparted by pre- and post-treatment of wool and acrylic using metal oxides nanoparticles to improve the printing properties of the treated fabrics. This study demonstrated the enhancement of the UV-shielding, self-cleaning and microbial protection of the treated fabrics. The printing pastes were formulated using composites of TGPLA or CLMA as thickening agents. The triglyceride polylactic acid thickening agent was prepared via thermal condensation process employing of glycerol and lactic acid at the molar ratio of 98:2 and in presence of sulfuric acid as a catalyst. The carboxy lactic methacrylate thickener was synthesized in one-pot polycondensation/free-radical reaction procedure from a mixture of lactic acid (98%) and methacrylic acid (2%) in presence of sulfuric acid as a catalyst. *N,N*-methylene diacrylamide was added as a cross-linking agent via free-radical reaction process in presence of potassium persulfate initiator [44,45]. Pre- and post-treated fabrics were exposed to screen-printing using either acid or basic dyestuffs followed by thermal fixation, washing and finally air-drying. The UV shielding, photocatalytic self-clean, antibacterial performance, color strength as well as the colorfastness properties of the screen-printed fabrics was evaluated. To achieve this goal, the synthesized titanium dioxide, magnesium oxide, and zinc oxide nanoparticles were synthesized according to previously reported procedures [46]. The fabrics were treated with TiO_2, MgO, and ZnO nanoparticles by the exhaustion procedure before and after the screen-printing process. The targeted fabrics (liquor ratio at 1:30) were padded at 80 °C for 20 min in an aqueous bath of the prepared nanoparticles at four different concentrations including 0.5%, 1.0%, 1.5%, 2.0% owf. To facilitate a homogenous dispersion of the metal oxide nanoparticles in the aqueous bath, a dispersing agent was added. The fabrics were then subjected to curing at 140 °C (TiO_2 and ZnO) or at 120 °C (MgO).

3.2. Morphology and Chemical Composition Properties

Scanning electron microscopic (SEM) analysis was applied to investigate the nano-structures of the metal oxides nanoparticles (concentration at 1.0% owf) and textile fibers, respectively. Both size and distribution of nanoparticles were also explored as shown in Figures 3–9. Energy-dispersive X-ray analysis (EDX) was applied to study the elemental composition of the treated fabrics (concentration of metal oxides nanoparticles at 1.0% owf) as shown in Figures 3–9. This technique was utilized to determine particularly the essential nanoparticles elements including ZnO, TiO_2 and MgO. Figure 3 showed SEM-EDX spectral analysis of the blank untreated wool fabric where there was no evidence of nanoparticles of metal oxides. Figure 4 displays the evidence of the metal oxide nanoparticles

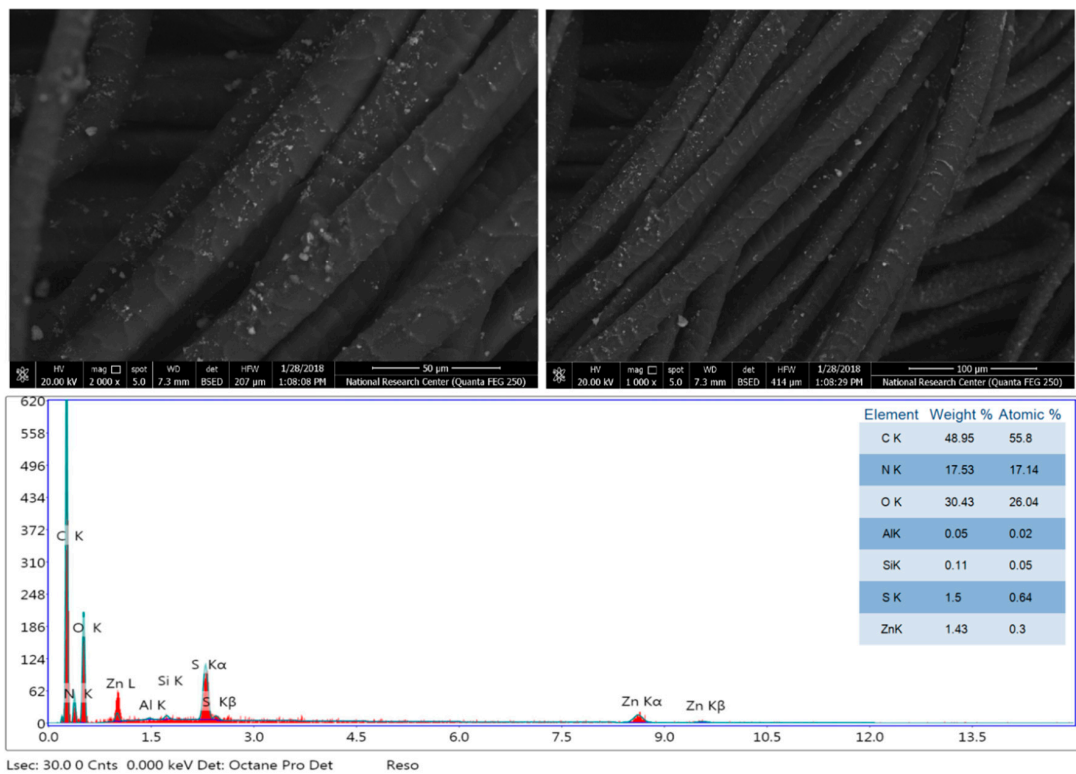monitored at low intensity due to the presence of Mg and O representing MgO structure. It was proved that magnesium combined with oxygen in the nano-scale according to the particle size in the SEM image. The presence of Zn and O atoms due to ZnO nanoparticles was confirmed in the pretreated wool sample (Figure 5), while the post-treated wool sample using ZnO nanoparticles is shown in Figure 6. SEM-EDX spectral analysis of the blank untreated acrylic fabric displaying no evidence of the presence of metal oxide nanoparticles as demonstrated in Figure 7. On the other hand, Figures 8 and 9 show the pre- and post-treated acrylic fabrics using TiO_2 and MgO nanoparticles, respectively. Figure 8 displays SEM-EDX spectra proving the existence of titanium element which confirmed the presence of TiO_2 nanoparticles incorporated onto the acrylic fabric surface. Similarly, Figure 9 displays acrylic fabric post-treated with MgO nanoparticles. The major elements were recorded at a high percentage. For example, carbon, sulfur, nitrogen and oxygen were found to be the major elements for wool fibers. However, other elements were monitored at a very low concentration, such as Al, Si, Na, Ca, K and Cl. Those traces of elements can be attributed to the other components and salts used in the printing paste. For example, the sodium element is due to the used Ludigol (the sodium salt of *m*-nitrobenzene sulfonic acid). Also, the EDX method is an excellent detection approach for all elements with a certain little error [53,54]. Similarly, the major elements for acrylic fibers, including carbon, oxygen and nitrogen, were recorded at a high percentage. However, the sulfur element was monitored at a very low concentration because EDX is an elemental detection technique with a certain small error [53,54]. Close assessment of the scanning electron microscope images displayed an average particle size in the range of approximately 50–100 nm for the treated wool/acrylic samples. No significant differences in the morphological properties were monitored upon changing the type or concentration of metal oxide nanoparticles. Similarly, no changes were detected upon changing the thickening agent (TGPLA or CLMA) or changing the fabric nature (wool or acrylic).
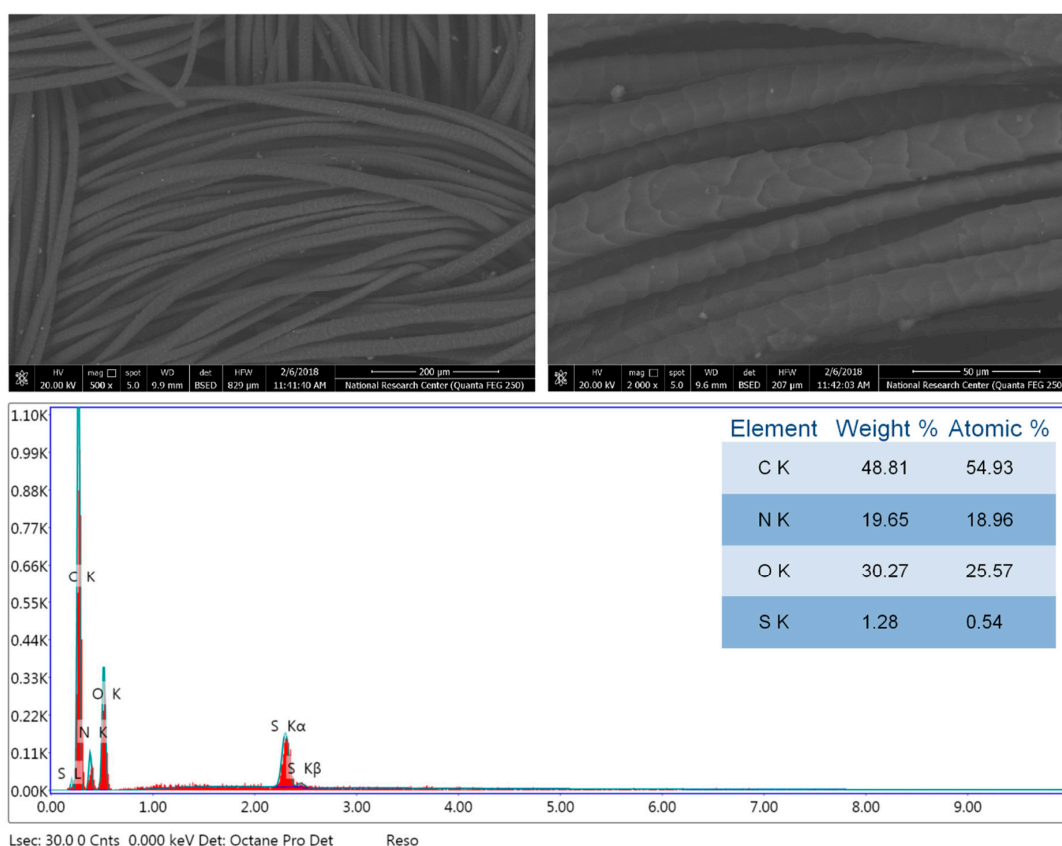
Figure 3. Scanning electron microscope (SEM) images and energy-dispersive X-ray analysis (EDX) diagram of blank/untreated wool fabric.

Element	Weight %	Atomic %
C K	55.45	63.64
O K	40.1	34.56
MgK	0.29	0.16
S K	2.39	1.03
CaK	1.77	0.61

Lsec: 30.0 0 Cnts 0.000 keV Det: Octane Pro Det　　　　Reso
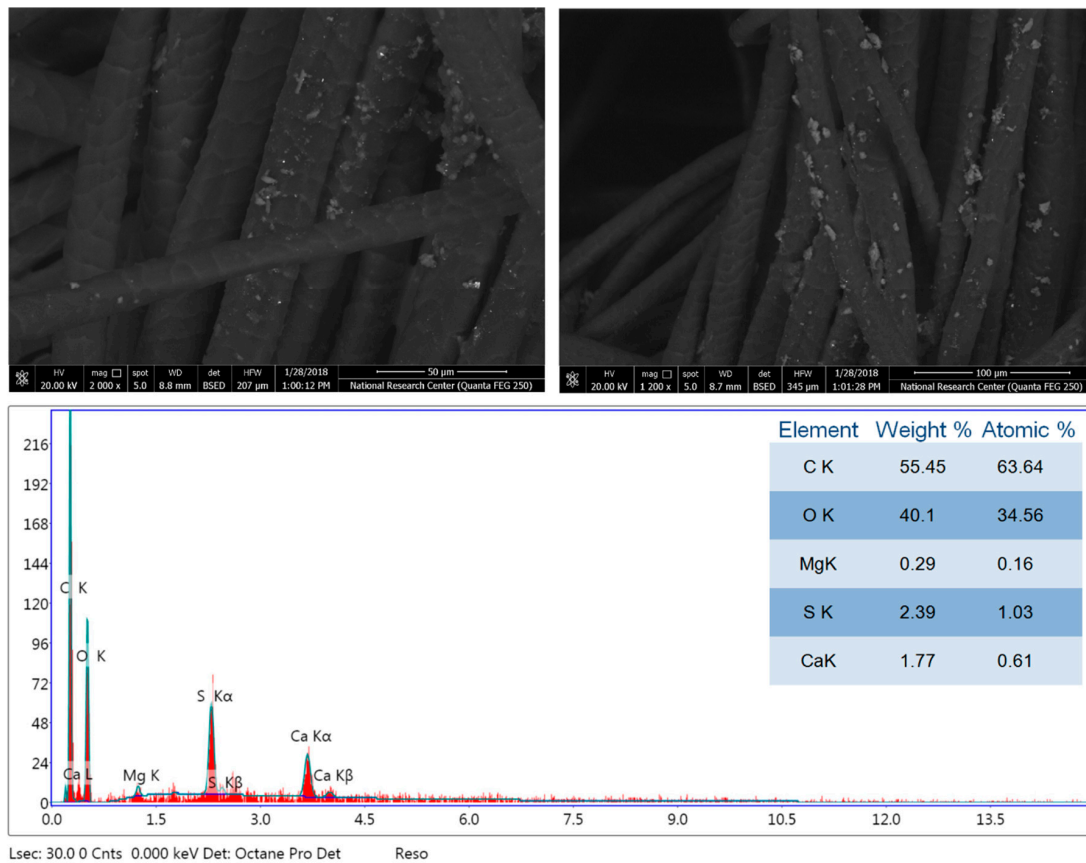
Figure 4. SEM images and EDX diagram of MgO nanoparticles incorporated onto a pre-treated wool fabric.

Element	Weight %	Atomic %
C K	48.95	55.8
N K	17.53	17.14
O K	30.43	26.04
AlK	0.05	0.02
SiK	0.11	0.05
S K	1.5	0.64
ZnK	1.43	0.3

Lsec: 30.0 0 Cnts 0.000 keV Det: Octane Pro Det　　　　Reso

Figure 5. SEM images and EDX diagram of ZnO nanoparticles immobilized onto a pre-treated wool fabric.

Element	Weight %	Atomic %
C K	46.58	53.09
N K	20.09	19.63
O K	30.78	26.33
NaK	0.02	0.01
S K	1.86	0.8
ZnK	0.67	0.14

Figure 6. SEM images and EDX diagram of ZnO nanoparticles post-treated wool fabric screen-printed with C.I. Acid Red 88.

Element	Weight %	Atomic %
C K	67.55	71.41
N K	25.71	23.3
O K	6.59	5.23
S K	0.15	0.06

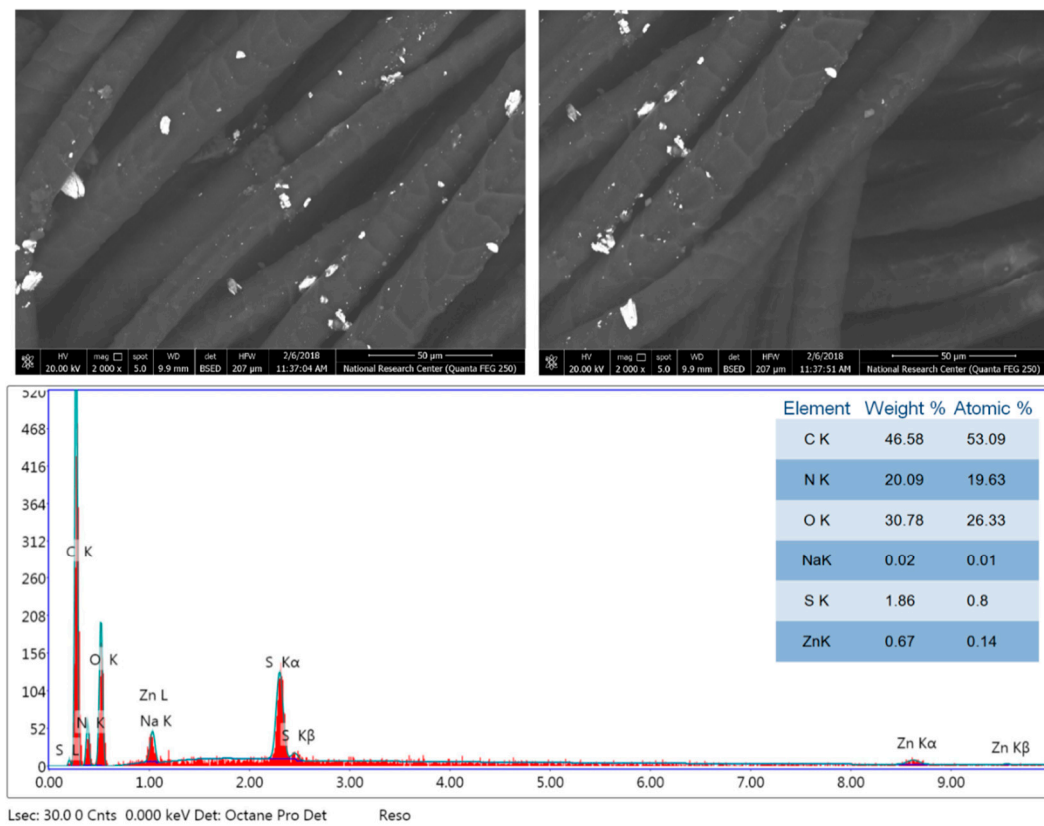**Figure 7.** SEM images and EDX diagram of blank/untreated acrylic fabric.
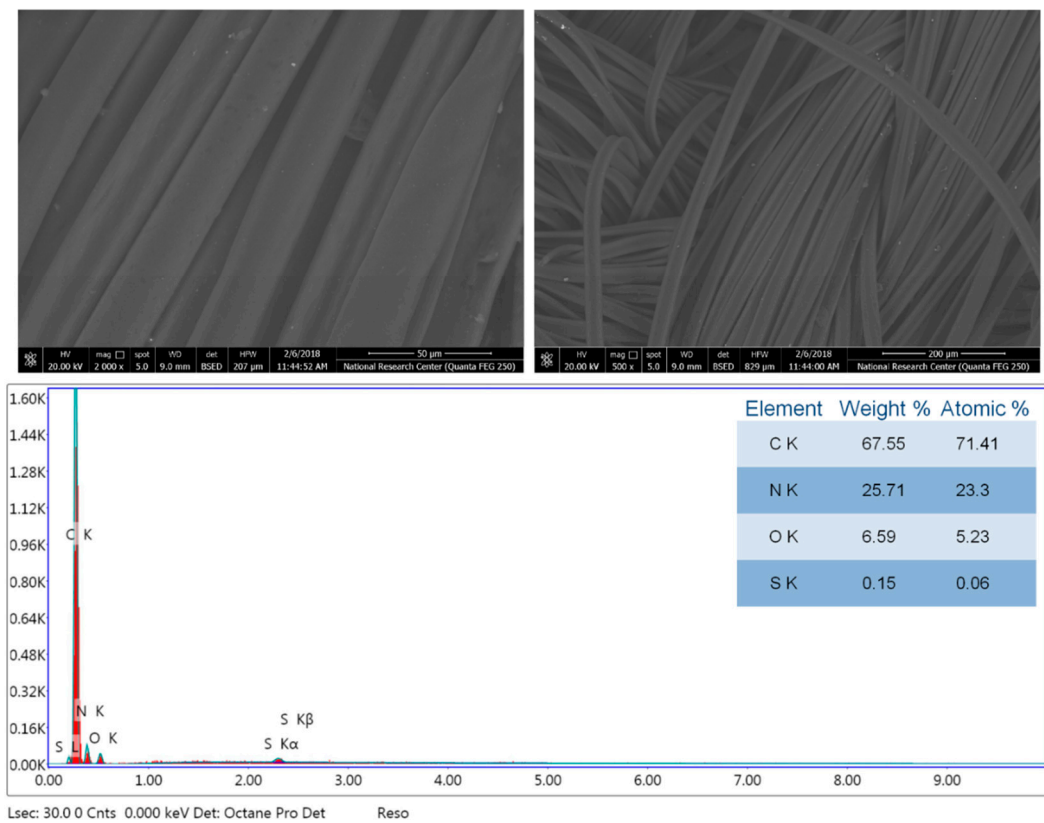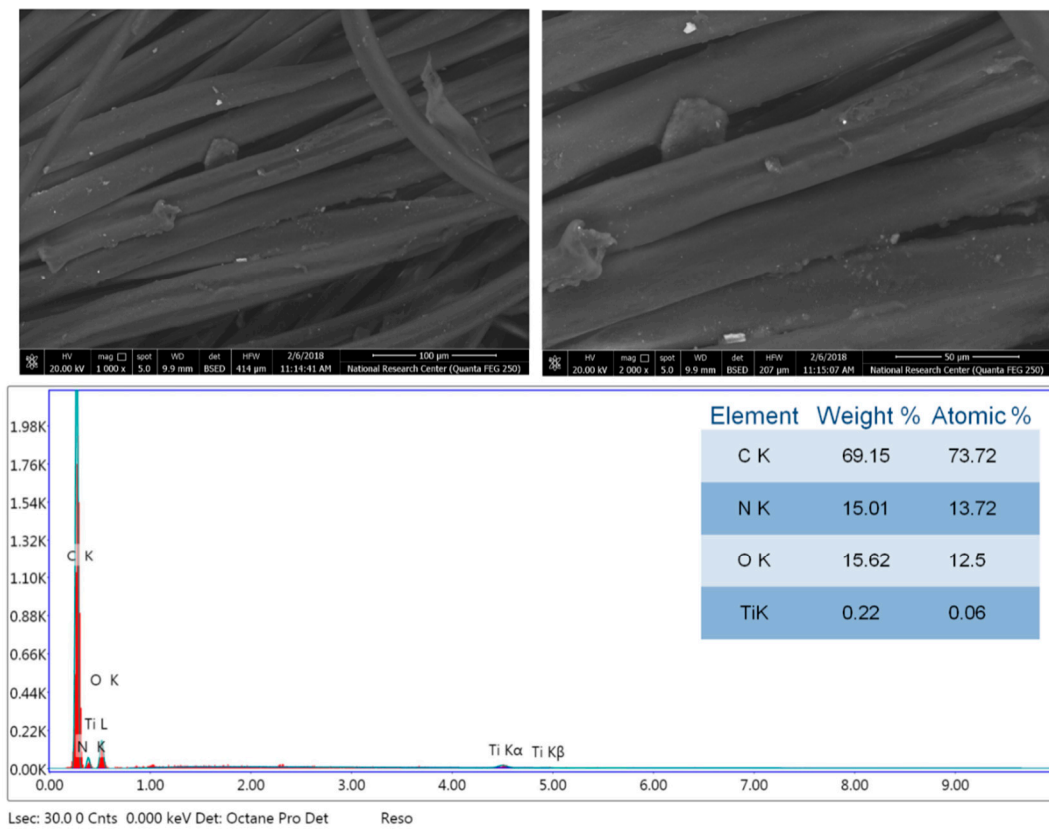
Figure 8. SEM images and EDX diagram of TiO$_2$ nanoparticles loaded onto a pre-treated acrylic fabric.
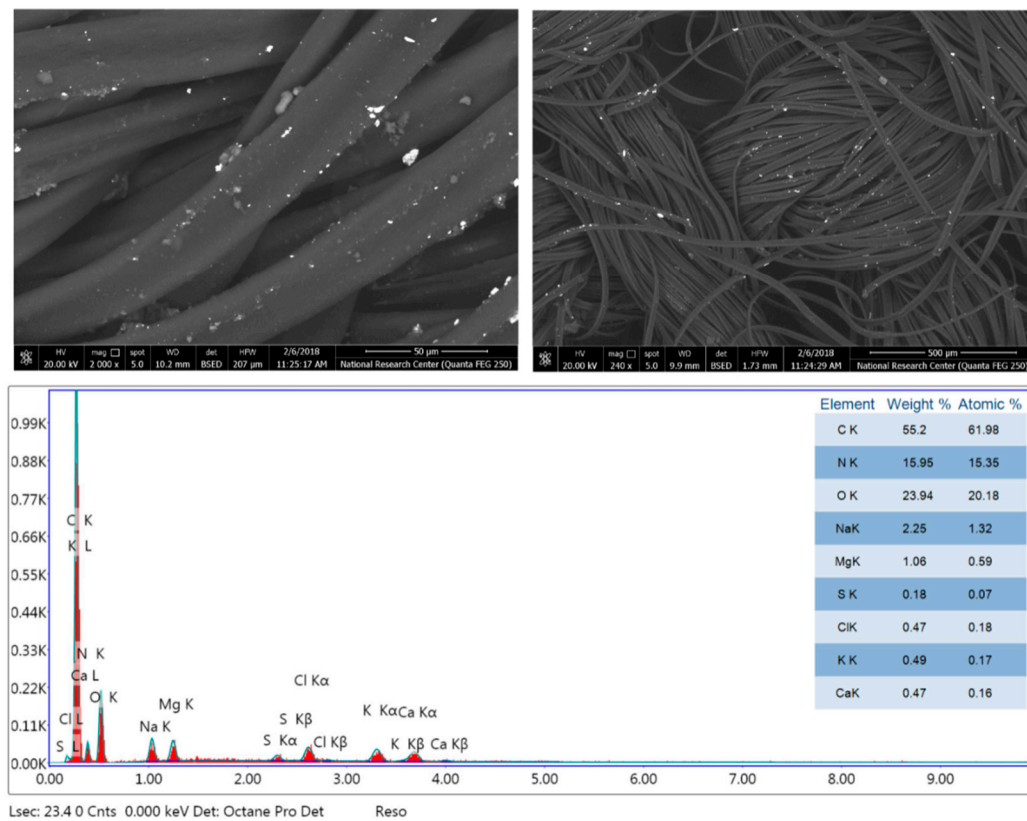

Figure 9. SEM images and EDX diagram of MgO nanoparticles deposited onto a post-treated acrylic fabric screen-printed with C.I. Basic Yellow 28.

3.3. Color Strength and Fastness Properties

Nanomaterials exhibit considerably novel and enhanced chemical, physical and biological characteristics as a result of their nano-scaled structure. To study those functional properties, both wool and acrylic fabrics were treated with ZnO, MgO and TiO$_2$ nanoparticles before and after screen printing. Four different concentrations (0.5, 1, 1.5 and 2% owf) were applied to optimize the most appropriate concentration for each metal oxide nanoparticles. To determine the effects of treating wool natural fibers on color strength (Table 3), samples were treated with metal oxide nanoparticles before and after the screen-printing process using C.I. Acid Red 88. The color strength of the treated wool fabrics was found to depend on the type and concentration of the metal oxide nanoparticles as well as the applied method itself if it was pre- or post-treatment. Upon increasing the concentration of metal oxide nanoparticles in the case of pre-treatment, the color strength values were found to decrease significantly with TiO$_2$, moderately decrease with ZnO, and moderately increase with MgO nanoparticles. When increasing the concentration of metal oxide nanoparticles in case of post-treatment, the color strength was found to moderately increase with ZnO, moderately decrease with MgO and slightly decrease with TiO$_2$ nanoparticles. The highest color strength value for the treated wool fabrics was monitored with TiO$_2$ nanoparticles at the lowest concentration. This proved that treating the wool fabric with lower concentration of titanium dioxide (0.5%) is adequate to accomplish a significant increase in the color strength. The increased color strength monitored at lower concentration of titanium dioxide could be attributed to Ti^{+4} ions which led to increasing positive charges causing more ionic attraction to the acid anionic dyestuffs and increasing the bonding process between dyestuff and fabric. However, the increased concentration of titanium dioxide nanoparticles higher than 0.5% (from 1%, 1.5% to 2% owf) resulted in a slight decrease in color strength, which could be attributed to the extensive increase in positive charges with high repulsion forces with each other's decreasing the bonding process between dyestuff and fabric [20,33,46]. Thus, the optimized conditions for the application of TiO$_2$ nanoparticles were found to be at the lower content (0.5% owf) for the pre-treatment process. All treated fabrics displayed slightly higher color strength compared to the control fabrics which were printed without treatment with nanoparticles. In general, the pre-treatment procedure displayed higher color strength compared to the post-treatment process. This is could be attributed to metal cations which increase the bonding process between dyestuff and the pre-treated fabric. On the other side, the post-treated fabric does not contain metal cations to support the bonding process between dyestuff and fabric during the printing process [34,37,46]. The color strength was found to increase in the pre-treatment process with the order of TiO$_2$ > ZnO > MgO at 0.5% owf total content of nanoparticles, while the post-treated fabrics exhibited the order of MgO > TiO$_2$ > ZnO.

Table 3. Effect of pre- and post-treatment of wool fabrics with different metal oxide nanoparticles on color strength using C.I. Acid Red 88 and triglyceride polylactic acid (TGPLA) thickener.

Metal Oxide Nanoparticles	Concentration	Color Strength (*K/S*)	
	(% owf)	Pre-Treatment	Post-Treatment
Control *	0	6.26	6.26
ZnO	0.5	11.19	5.45
	1.0	10.25	7.25
	1.5	6.58	9.06
	2.0	5.18	10.48
MgO	0.5	9.45	10.4
	1.0	11.57	7.98
	1.5	12.11	7.21
	2.0	13.28	6.63
TiO$_2$	0.5	15.07	8.57
	1.0	14.38	8.43
	1.5	14.28	7.69
	2.0	7.93	7.53

* Control fabrics are printed fabrics but untreated with nanoparticles.

Similarly, both pre- and post-treatment procedures on color strength of screen-printed acrylic fabrics using C.I. Basic Yellow 28 and carboxy lactic methacrylate (CLMA) thickener were investigated (Table 4). When increasing the content of metal oxide nanoparticles in the pre-treatment process, the color strength was moderately decreased with ZnO, moderately increased with MgO and significantly decreased with TiO$_2$ nanoparticles. Upon increasing the total content of the nanoparticles in the post-treatment process, the color strength moderately decreased with TiO$_2$, slightly increased with MgO and moderately increased with ZnO nanoparticles. The best color strength was monitored with ZnO nanoparticles at the lowest total content of nanoparticles (0.5%), which could be considered the optimized conditions for the application of ZnO nanoparticles on acrylic fibers that had undergone the pre-treatment process. All treated acrylic fibers demonstrated almost better color strength compared to the control acrylic fibers. Generally, the pre-treatment approach demonstrated better color strength values compared to the post-treatment method [46]. Additionally, the color strength increased in the pre-treatment approach in the order ZnO > TiO$_2$ > MgO at 0.5% owf, while the post-treated samples demonstrated the order TiO$_2$ > MgO > ZnO. However, the enhanced color strength values on acrylic fabrics was less than that on wool owing to the higher accumulation of positive charges on wool compared to acrylic fibers.

Table 4. Effect of pre- and post-treatment of acrylic fabrics with different metal oxide nanoparticles on color strength of printed fabrics using C.I. Basic Yellow 28 and carboxy lactic methacrylate (CLMA) thickener.

Metal Oxide Nanoparticles	Concentration	*K/S*	
	(% owf)	Pre-Treatment	Post-Treatment
Control *	0	13.99	13.99
ZnO	0.5	18.66	14.39
	1.0	16.54	15.78
	1.5	14.61	16.82
	2.0	14.32	17.2
MgO	0.5	14.54	15.27
	1.0	16.51	15.36
	1.5	16.78	16.75
	2.0	17.43	16.96
TiO$_2$	0.5	17.64	15.3
	1.0	16.4	13.77
	1.5	11.37	13.38
	2.0	10.45	12.9

* Control fabrics are printed fabrics but untreated with nanoparticles.

The effects of pre- and post-treating wool and acrylic fibers with metal oxide nanoparticles on the colorfastness properties using acid or basic dyestuff based prints were investigated. The printed samples with the highest color strength were selected and subjected to overall colorfastness measurements as shown in Table 5. The fastness properties slightly depended on the type of dyestuff and fabric as well as the type and concentration of the applied nanoparticles in either pre- or post-treatment fabrics. However, it is also obvious that the colorfastness properties for all prints were nearly equal or slightly higher than the control fabric.

3.4. Antibacterial Performance of Treated and Untreated Fabrics

The antimicrobial activity can be imparted to a textile product by chemical or physical integration of active agents onto this textile product [28–31]. Tables 6 and 7 demonstrated the antibacterial performance of wool and acrylic fabrics depending on the type and total content of metal oxide nanoparticles. The highest antibacterial efficiency in preventing infection was monitored upon using TiO$_2$ compared to ZnO and MgO nanoparticles. No antibacterial activity was monitored for the

untreated/blank wool and acrylic fabrics. Wool pre-treated with TiO_2 nanoparticles demonstrated higher reduction of bacterial count% due to the efficient photocatalytic influence of TiO_2 nanoparticles. Upon exposure to light, photons with energy higher than the bond-gap of TiO_2 stimulate electrons up to the conduction-band. Those excited electrons inside the crystal structural system interact with the air oxygen generating free radical oxygen atoms with an oxidizing ability to break down the bacterial cell wall via an oxidation/reduction process. On the other side, the antibacterial activity of ZnO nanoparticles rising from the induction of oxidation stress owing to the production of active oxygen species with the ability to degrade the bacterial cell membrane. According to the close values of the antibacterial activities displayed in Tables 6 and 7, the nature of the employed thickener and dyestuff had no influence on the antibacterial performance of the treated fabrics.

Table 5. Colorfastness properties of wool and acrylic fibers pre- and post-treated with nanoparticles and printed with acid or basic dyestuffs employing TGPLA or CLMA thickeners, respectively.

| Conditions | Metal Oxides NP$_s$ | Dye | Rubbing | | Washing | | Perspiration | | | | Light |
| | | | Wet | Dry | St. | Alt. | Acidic | | Alkaline | | |
							St.	Alt.	St.	Alt.	
Wool/TGPLA Pre-treatment	Control	Acid dye	4	3–4	4	4	4	4–5	4	4	6–7
	ZnO/0.5%		4	3–4	4	4	4	4–5	4	4	6–7
	MgO/2.0%		4	3–4	4	4	4	4	4	4	7
	TiO$_2$/0.5%		3–4	3	4	4	3–4	3–4	4	4	6–7
Wool/TGPLA Post-treatment	Control		3–4	3	4	4	3–4	4	4	4	7
	ZnO/2.0%		4	3–4	4	4	4	4	4	4	6–7
	MgO/0.5%		4	3–4	4	4	4	4–5	4	4	7
	TiO$_2$/0.5%		4	3–4	4	4	4	4–5	4	4	6–7
Acrylic/CLMA Pre-treatment	Control	Basic dye	4	3–4	4	4	4	4–5	4	4	6–7
	ZnO/0.5%		4	3–4	4	4	4	4–5	4	4	6–7
	MgO/2.0%		4	4	4	4	4	4	4	4	6–7
	TiO$_2$/0.5%		4	3–4	4	4	4	4	4	4	7
Acrylic/CLMA Post-treatment	Control		3–4	3	4	4	3–4	3–4	4	4	6–7
	ZnO/2.0%		3–4	3	4	4	3–4	4	4	4	7
	MgO/2.0%		4	3–4	4	4	4	4	4	4	7
	TiO$_2$/0.5%		4	3–4	4	4	4	4	4	4	6–7

St.: Staining (cotton), Alt.: Alteration; light fastness was evaluated by international blue scale (1 and 2-very poor, 3-poor, 4-fair, 5-good, 6 and 7-very good and 8-excellent); washing, perspiration and rubbing was assessed by international grey scale (1-very poor, 2-poor, 3-fair, 4-very good and 5-excellent).

Table 6. Antibacterial performance of unprinted wool and acrylic fabrics treated with metal oxide nanoparticles.

| Sample | | *E. Coli* (G−) | | *S. Aureus* (G+) | |
		Wool	Acrylic	Wool	Acrylic
Untreated/Blank		0.0	0.0	0.0	0.0
MgO	0.5%	27	30	37	30
	1.5%	27	32	39	26
	2.0%	30	32	39	20
TiO$_2$	0.5%	31	36	40	36
	1.5%	30	37	40	27
	2.0%	29	34	38	27
ZnO	0.5%	30	32	37	29
	1.5%	26	32	37	28
	2.0%	29	30	36	26

Table 7. Antibacterial activity for the printed wool (TGPLA and acid dyestuff) and acrylic (CLMA and basic dyestuff) fabrics pre- and post-treated with metal oxide nanoparticles.

Sample		Pre-Treatment		Post-Treatment	
		S. aureus (G+)	*E. coli (G−)*	*S. aureus (G+)*	*E. coli (G−)*
Control		0	0	0	0
Wool (TiO$_2$)	0.50%	30	36	31	39
	1.00%	40	34	26	36
	1.50%	38	36	27	37
	2.00%	30	31	20	33
Wool (MgO)	0.50%	28	37	27	37
	1.00%	26	32	24	25
	1.50%	28	35	26	36
	2.00%	31	37	29	37
Wool (ZnO)	0.50%	29	40	18	33
	1.00%	28	32	26	34
	1.50%	25	33	32	38
	2.00%	24	35	29	39
Acrylic (TiO$_2$)	0.50%	35	32	24	32
	1.00%	34	34	26	36
	1.50%	30	32	28	36
	2.00%	36	35	28	39
Acrylic (MgO)	0.50%	28	31	27	34
	1.00%	26	32	24	25
	1.50%	24	32	21	34
	2.00%	25	34	25	36
Acrylic (ZnO)	0.50%	22	31	28	35
	1.00%	28	32	26	34
	1.50%	25	32	27	31
	2.00%	21	32	24	30

3.5. Ultraviolet Protection Activity

The ultraviolet radiation shielding properties of pristine, treated unprinted and pre/post-treated printed wool (acid dyestuff and TGPLA thickener) and acrylic (basic dyestuff and CLMA thickener) fabrics were explored by absorbance spectroscopy. Each value was an average of three readings carried out by rotating the fabric by 90°. The transmission results were employed to determine the ultraviolet protection factor (UPF) and the percentage of the ultraviolet transmission. Table 8 displays the ultraviolet protection values after irradiation. The results designated that most treated samples exhibited satisfactory ultraviolet protection compared to the pristine (unprinted and untreated with nanoparticles; 49.8 for wool and 45.6 for acrylic) and controlled (printed and untreated with nanoparticles; 57.3 for wool and 51.7 for acrylic) fabrics. All printed and unprinted fabrics treated with ZnO, MgO and TiO$_2$ nanoparticles demonstrated a slight enhancement in the ultraviolet shielding effect compared to the pristine fabric. However, the pre- and post-treated printed samples displayed a slightly higher UV shielding efficiency, particularly for the post-treated wool samples. In general, the UV protection the post-treated printed samples were found to increase with increasing the concentration of the metal oxide nanoparticles. Similarly, the unprinted/treated and printed/pre-treated wool/MgO, printed/pre-treated acrylic/TiO$_2$, and unprinted/treated acrylic/ZnO samples were found to increase by increasing the concentration of the metal oxide nanoparticles. On the contrary, the unprinted/treated and printed/pre-treated wool/TiO$_2$, wool/ZnO and acrylic/MgO samples were found to decrease by increasing the concentration of the metal oxide nanoparticles. Similarly, the unprinted/treated acrylic/TiO$_2$ and printed/pre-treated fabrics were found to decrease by increasing the concentration of

the metal oxide nanoparticles. The screen-printed post-treated wool with the highest content of TiO_2 displayed the best UV blocking values.

Table 8. Ultraviolet (UV) blocking of nanoparticles-immobilized unprinted and printed (pre- and post-treated) wool (acid dyestuff and TGPLA thickener) and acrylic (basic dyestuff and CLMA thickener) fabrics after irradiation.

Sample		Ultraviolet Protection Factor (UPF)		
		Unprinted	Printed	
			Pre-Treated	Post-Treated
Wool (TiO$_2$)	0.5	143.3	152.2	160.5
	1.0	145.4	149.8	165.2
	1.5	144.3	145.0	167.8
	2.0	140.9	139.1	177.6
Wool (MgO)	0.5	135.2	76.6	92.7
	1.0	141.5	102.9	117.1
	1.5	147.0	105.7	122.3
	2.0	148.7	108.2	125.2
Wool (ZnO)	0.5	166.5	135.8	84.6
	1.0	153.6	111.7	109.3
	1.5	123.8	90.0	124.1
	2.0	99.4	72.3	157.2
Acrylic (TiO$_2$)	0.5	136.8	111.5	129.0
	1.0	132.4	118.2	139.5
	1.5	126.7	121.6	144.8
	2.0	108.5	126.4	151.3
Acrylic (MgO)	0.5	92.5	78.0	67.6
	1.0	91.0	69.3	73.9
	1.5	78.7	61.5	82.0
	2.0	76.9	57.4	94.5
Acrylic (ZnO)	0.5	77.5	59.1	51.7
	1.0	83.6	51.7	55.4
	1.5	105.8	47.9	68.4
	2.0	119.9	43.2	79.0

3.6. Self-Cleaning Activity

One of the significant properties of metal oxide nanoparticles treatment is the conversion of the absorbed light into self-cleaning materials with the ability to degrade its stain [14]. Table 9 showed the influence of methylene blue on the pre- and post-treated printed fabrics with metal oxide nanoparticles using either TGPLA or CLMA thickener after 12 h of ultraviolet illumination. The pre- and post-treatment of wool and acrylic samples resulted in the formation of nanoparticles thin film with the ability to increase the hydrophobic properties of the fabric surface as a consequence of the Lotus effect. Generally, metal oxide nanoparticles employ a distinctive self-cleaning mechanism by combining an initial photocatalysis with a subsequent hydrophobic step. Upon exposure to ultraviolet light, metal oxide nanoparticles produce free electrons which interact with oxygen and water molecules in the air to generate free radicals. Those free radicals have the ability to degrade organic matter fouling on the fabric surface. Due to the hydrophobic effect generated by the metal oxide nanoparticles on the fabric surface, water can then wash the fabric surface from any surface debris [14,55,56].

Table 9. Self-cleaning activity of wool and acrylic samples screen-printed with CLMA or TGPLA thickening agents and pre/post-treated with metal oxide nanoparticles.

Sample		Dye Removal %	
		Post-Treatment	Pre-Treatment
		Basic Dyestuff (CLMA)	
Acrylic (TiO$_2$)	0.5	90%	95%
	1.0	90%	90%
	1.5	95%	80%
	2.0	90%	90%
Acrylic (MgO)	0.5	90%	90%
	1.0	80%	90%
	1.5	90%	90%
	2.0	90%	80%
Acrylic (ZnO)	0.5	90%	90%
	1.0	80%	90%
	1.5	90%	90%
	2.0	90%	85%
		Acid Dyestuff(TGPLA)	
Wool (TiO$_2$)	0.5	90%	90%
	1.0	85%	90%
	1.5	90%	90%
	2.0	90%	90%
Wool (MgO)	0.5	90%	90%
	1.0	85%	90%
	1.5	70%	95%
	2.0	80%	90%
Wool (ZnO)	0.5	90%	90%
	1.0	90%	95%
	1.5	90%	95%
	2.0	80%	90%

4. Conclusions

In summary, we describe a new method for the production of printed smart textiles with multifunctional properties. Three metal oxides nanoparticles (ZnO, MgO and TiO$_2$) were prepared and applied to wool and acrylic fibers at different concentrations before and after running the printing process. The printing pastes were formulated using acid or basic dyestuffs as well as triglyceride polylactic acid (TGPLA) or carboxy lactic methacrylate (CLMA) as thickening agents. Both scanning electron microscopy (SEM) and energy-dispersive X-ray analysis (EDX) of the printed textile substrates were described. The printed fabrics were found to exhibit antimicrobial activity, UV protection, and good colorfastness properties. Both pre- and post-treated fabrics introduced a thin film of nanoparticles with the ability to increase the fabric hydrophobic performance leading to better photocatalytic self-cleaning activity. Furthermore, the color strength properties were found to be improved. The presence of nanoparticles on the fabric surface during the printing course significantly increased the fabric color strength which depended mainly on the type and concentration of the metal oxide nanoparticles. These results suggest that metal oxides nanoparticles could establish ideal multifunctional prints for technical textiles production. Thus, the application of nanocomposites to textile fibers can afford multifunctional fabrics with enhanced printing properties. The metal oxides, such as TiO$_2$, MgO and ZnO are particularly attractive due to their stability under harsh circumstances. They are also non-toxic for humans.

References

1. Milwich, M.; Speck, T.; Speck, O.; Stegmaier, T.; Planck, H. Biomimetics and technical textiles: Solving engineering problems with the help of nature's wisdom. *Am. J. Bot.* **2006**, *93*, 1455–1465. [CrossRef] [PubMed]

2. Reinhart, G.; Straßer, G. Flexible gripping technology for the automated handling of limp technical textiles in composites industry. *Prod. Eng.* **2011**, *5*, 301–306. [CrossRef]

3. Khattab, T.A.; Fouda, M.M.; Abdelrahman, M.S.; Othman, S.I.; Bin-Jumah, M.; Alqaraawi, M.A.; Fassam, H.A.; Allam, A.A. Co-encapsulation of enzyme and tricyanofuran hydrazone into alginate microcapsules incorporated onto cotton fabric as a biosensor for colorimetric recognition of urea. *React. Funct. Polym.* **2019**, *142*, 199–206. [CrossRef]

4. Ma, C.; Zhao, S.; Huang, G. Anti-static charge character of the plasma treated polyester filter fabric. *J. Electrost.* **2010**, *68*, 111–115.

5. Abdelrahman, M.S.; Tawfik, A.K. Development of One-Step Water-Repellent and Flame-Retardant Finishes for Cotton. *ChemistrySelect* **2019**, *4*, 3811–3816. [CrossRef]

6. Huang, J.Y.; Li, S.H.; Ge, M.Z.; Wang, L.N.; Xing, T.L.; Chen, G.Q.; Liu, X.F. Robust superhydrophobic TiO 2@ fabrics for UV shielding, self-cleaning and oil–water separation. *J. Mater. Chem. A* **2015**, *3*, 2825–2832. [CrossRef]

7. Khattab, T.A.; Mowafi, S.; El-Sayed, H. Development of mechanically durable hydrophobic lanolin/silicone rubber coating on viscose fibers. *Cellulose* **2019**, *26*, 9361–9371. [CrossRef]

8. Zheng, X.; Guo, Z.; Tian, D.; Zhang, X.; Li, W.; Jiang, L. Underwater self-cleaning scaly fabric membrane for oily water separation. *ACS Appl. Mater. Interfaces* **2015**, *7*, 4336–4343. [CrossRef] [PubMed]

9. Yetisen, A.K.; Qu, H.; Manbachi, A.; Butt, H.; Dokmeci, M.R.; Hinestroza, J.P.; Skorobogatiy, M.; Khademhosseini, A.; Yun, S.H. Nanotechnology in textiles. *ACS Nano* **2016**, *10*, 3042–3068. [CrossRef] [PubMed]

10. Khattab, T.A.; Kassem, N.F.; Adel, A.M.; Kamel, S. Optical Recognition of Ammonia and Amine Vapor Using "Turn-on" Fluorescent Chitosan Nanoparticles Imprinted on Cellulose Strips. *J. Fluoresc.* **2019**, *29*, 693–702. [CrossRef]

11. Lund, A.; van der Velden, N.M.; Persson, N.K.; Hamedi, M.M.; Müller, C. Electrically conducting fibres for e-textiles: An open playground for conjugated polymers and carbon nanomaterials. *Mater. Sci. Eng. R Rep.* **2018**, *126*, 1–29. [CrossRef]

12. Hu, L.; Cui, Y. Energy and environmental nanotechnology in conductive paper and textiles. *Energy Environ. Sci.* **2012**, *5*, 6423–6435. [CrossRef]

13. Dastjerdi, R.; Montazer, M. A review on the application of inorganic nano-structured materials in the modification of textiles: Focus on anti-microbial properties. *Colloids Surf. B Biointerfaces* **2010**, *79*, 5–18. [CrossRef] [PubMed]

14. Rehan, M.; Barhoum, A.; Khattab, T.A.; Gatjen, L.; Wilken, R. Colored, photocatalytic, antimicrobial and UV-protected viscose fibers decorated with Ag/Ag_2CO_3 and Ag/Ag_3PO_4 nanoparticles. *Cellulose* **2019**, *26*, 5437–5453. [CrossRef]

15. Avila, A.G.; Juan, P. Hinestroza. Smart textiles: Tough cotton. *Nat. Nanotechnol.* **2008**, *3*, 458. [CrossRef]

16. Mitrano, D.M.; Rimmele, E.; Wichser, A.; Erni, R.; Height, M.; Nowack, B. Presence of nanoparticles in wash water from conventional silver and nano-silver textiles. *ACS Nano* **2014**, *8*, 7208–7219. [CrossRef]

17. Montazer, M.; Pakdel, E.; Behzadnia, A. Novel feature of nano-titanium dioxide on textiles: Antifelting and antibacterial wool. *J. Appl. Polym. Sci.* **2011**, *121*, 3407–3413. [CrossRef]

18. Shahid, M.; Mohammad, F. Green chemistry approaches to develop antimicrobial textiles based on sustainable biopolymers: A review. *Ind. Eng. Chem. Res.* **2013**, *52*, 5245–5260. [CrossRef]

19. Lee, H.J.; Yeo, S.Y.; Jeong, S.H. Antibacterial effect of nanosized silver colloidal solution on textile fabrics. *J. Mater. Sci.* **2003**, *38*, 2199–2204. [CrossRef]

20. Montazer, M.; Pakdel, E. Functionality of nano titanium dioxide on textiles with future aspects: Focus on wool. *J. Photochem. Photobiol. C Photochem. Rev.* **2011**, *12*, 293–303. [CrossRef]

21. Köhler, A.R.; Som, C. Risk preventative innovation strategies for emerging technologies the cases of nano-textiles and smart textiles. *Technovation* **2014**, *34*, 420–430. [CrossRef]

22. Becheri, A.; Dürr, M.; Nostro, P.L.; Baglioni, P. Synthesis and characterization of zinc oxide nanoparticles: Application to textiles as UV-absorbers. *J. Nanoparticle Res.* **2008**, *10*, 679–689. [CrossRef]

23. Toshniwal, L.; Fan, Q.; Ugbolue, S.C. Dyeable polypropylene fibers via nanotechnology. *J. Appl. Polym. Sci.* **2007**, *106*, 706–711. [CrossRef]

24. He, L.; Gao, C.; Li, S.; Chung, C.T.W.; John, H.X. Non-leaching and durable antibacterial textiles finished with reactive zwitterionic sulfobetaine. *J. Ind. Eng. Chem.* **2017**, *46*, 373–378. [CrossRef]

25. Chen, S.; Yuan, L.; Li, Q.; Li, J.; Zhu, X.; Jiang, Y.; Sha, O.; Yang, X.; Xin, J.H.; Wang, J. Durable antibacterial and nonfouling cotton textiles with enhanced comfort via zwitterionic sulfopropylbetaine coating. *Small* **2016**, *12*, 3516–3521. [CrossRef]

26. Kang, C.K.; Kim, S.S.; Kim, S.; Lee, J.; Lee, J.H.; Roh, C.; Lee, J. Antibacterial cotton fibers treated with silver nanoparticles and quaternary ammonium salts. *Carbohydr. Polym.* **2016**, *151*, 1012–1018. [CrossRef]

27. Zhang, S.; Yang, X.; Tang, B.; Yuan, L.; Wang, K.; Liu, X.; Zhu, X.; Li, J.; Ge, Z.; Chen, S. New insights into synergistic antimicrobial and antifouling cotton fabrics via dually finished with quaternary ammonium salt and zwitterionic sulfobetaine. *Chem. Eng. J.* **2018**, *336*, 123–132. [CrossRef]

28. Ibrahim, N.A.; El-Zairy, E.M.R.; Eid, B.M. Eco-friendly modification and antibacterial functionalization of viscose fabric. *J. Text. Inst.* **2017**, *108*, 1406–1411. [CrossRef]

29. Gu, J.; Yuan, L.; Zhang, Z.; Yang, X.; Luo, J.; Gui, Z.; Chen, S. Non-leaching bactericidal cotton fabrics with well-preserved physical properties, no skin irritation and no toxicity. *Cellulose* **2018**, *25*, 5415–5426. [CrossRef]

30. Feng, X.; Zheng, K.; Wang, C.; Chu, F.; Chen, Y. Durable antibacterial cotton fabrics with chitosan based quaternary ammonium salt. *Fibers Polym.* **2016**, *17*, 371–379. [CrossRef]

31. Mwafy, E.A.; Hasanin, M.S.; Mostafa, A.M. Cadmium oxide/TEMPO-oxidized cellulose nanocomposites produced by pulsed laser ablation in liquid environment: Synthesis, characterization, and antimicrobial activity. *Opt. Laser Technol.* **2019**, *120*, 105744. [CrossRef]

32. Soltani, R.D.C.; Safari, M.; Mashayekhi, M. Sonocatalyzed decolorization of synthetic textile wastewater using sonochemically synthesized MgO nanostructures. *Ultrason. Sonochemistry* **2016**, *30*, 123–131. [CrossRef] [PubMed]

33. Pulit-Prociak, J.; Chwastowski, J.; Kucharski, A.; Banach, M. Functionalization of textiles with silver and zinc oxide nanoparticles. *App. Surf. Sci.* **2016**, *385*, 543–553. [CrossRef]

34. Karimi, L.; Yazdanshenas, M.E.; Khajavi, R.; Rashidi, A.; Mirjalili, M. Functional finishing of cotton fabrics using graphene oxide nanosheets decorated with titanium dioxide nanoparticles. *J. Text. Inst.* **2016**, *107*, 1122–1134. [CrossRef]

35. Mwafy, E.A.; Mostafa, A.M. Multi walled carbon nanotube decorated cadmium oxide nanoparticles via pulsed laser ablation in liquid media. *Opt. Laser Technol.* **2019**, *111*, 249–254. [CrossRef]

36. Ibrahim, N.A.; Eid, B.M.; Khattab, T.A. Environmentally Sound Dyeing of Cellulose-Based Textiles. *Text. Cloth.* **2019**, 79–99. [CrossRef]

37. Petkova, P.; Francesko, A.; Perelshtein, I.; Gedanken, A.; Tzanov, T. Simultaneous sonochemical-enzymatic coating of medical textiles with antibacterial ZnO nanoparticles. *Ultrason. Sonochemistry* **2016**, *29*, 244–250. [CrossRef]

38. Babar, A.A.; Peerzada, M.H.; Jhatial, A.K. Pad ultrasonic batch dyeing of causticized lyocell fabric with reactive dyes. *Ultrason. Sonochemistry* **2017**, *34*, 993–999. [CrossRef]

39. Gaffer, H.; Khattab, T. Synthesis and characterization of some azo-heterocycles incorporating pyrazolopyridine moiety as disperse dyes. *Egypt. J. Chem.* **2017**, *60*, 41–47.

40. Li, Z.; Dong, Y.; Li, B.; Wang, P.; Chen, Z.; Bian, L. Creation of self-cleaning polyester fabric with TiO_2 nanoparticles via a simple exhaustion process: Conditions optimization and stain decomposition pathway. *Mater. Des.* **2018**, *140*, 366–375. [CrossRef]

41. OhadiFar, P.; Shahidi, S.; Dorranian, D. Synthesis of Silver Nanoparticles and Exhaustion on Cotton Fabric Simultaneously Using Laser Ablation Method. *J. Nat. Fibers* **2018**, 1–12. [CrossRef]

42. Khattab, T.A.; Allam, A.A.; Othman, S.I.; Bin-Jumah, M.; Al-Harbi, H.M.; Fouda, M.M. Synthesis, Solvatochromic Performance, pH Sensing, Dyeing Ability, and Antimicrobial Activity of Novel Hydrazone Dyestuffs. *J. Chem.* **2019**, *2019*. [CrossRef]

43. Velmurugan, P.; Shim, J.; Bang, K.S.; Oh, B.T. Gold nanoparticles mediated coloring of fabrics and leather for antibacterial activity. *J. Photochem. Photobiol. B Biol.* **2016**, *160*, 102–109. [CrossRef] [PubMed]

44. Abdelrahman, M.S.; Nassar, S.H.; Mashaly, H.; Mahmoud, S.; Maamoun, D.; Khattab, T.A. Polymerization products of lactic acid as synthetic thickening agents for textile printing. *J. Mol. Struct.* **2020**, *1203*, 127421. [CrossRef]

45. Abdelrahman, M.S.; Sahar, H.N.; Mashaly, H.; Mahmoud, S.; Maamoun, D. Synthesis and Characterization of Biodegradable Synthetic Thickener from Anionic Triglyceride Polylactic Acid. *Appl. Ecol. Environ. Sci.* **2018**, *6*, 35–47. [CrossRef]

46. El-Thalouth, J.; Abd, I.; Mashaly, H.M. Imparting Multi-Functional Performance on Cellulosic Fabrics via Nanotechnology. *Int. J. Innov. Appl. Stud.* **2016**, *18*, 140.

47. Khattab, T.A.; Elnagdi, M.H.; Haggaga, K.M.; Abdelrahmana, A.A.; Abdelmoez Aly, S. Green synthesis, printing performance, and antibacterial activity of disperse dyes incorporating arylazopyrazolopyrimidines. *AATCC J. Res.* **2017**, *4*, 1–8. [CrossRef]

48. Khattab, T.A.; Haggag, K.M.; Elnagdi, M.H.; Abdelrahman, A.A.; Abdelmoez Aly, S. Microwave-assisted synthesis of arylazoaminopyrazoles as disperse dyes for textile printing. *Z. Fur Anorg. Und Allg. Chem.* **2016**, *642*, 766–772. [CrossRef]

49. Rehan, M.; Ahmed-Farid, O.A.; Ibrahim, S.R.; Hassan, A.A.; Abdelrazek, A.M.; Khafaga, N.I.; Khattab, T.A. Green and sustainable encapsulation of Guava leaf extracts (*Psidium guajava*, L.) into alginate/starch microcapsules for multifunctional finish over cotton gauze. *ACS Sustain. Chem. Eng.* **2019**, *7*, 18612–18623. [CrossRef]

50. Khan, R.; Fulekar, M.H. Biosynthesis of titanium dioxide nanoparticles using Bacillus amyloliquefaciens culture and enhancement of its photocatalytic activity for the degradation of a sulfonated textile dye Reactive Red 31. *J. Colloid Interface Sci.* **2016**, *475*, 184–191. [CrossRef]

51. Khattab, T.A.; Fouda, M.M.; Abdelrahman, M.S.; Othman, S.I.; Bin-Jumah, M.; Alqaraawi, M.A.; Fassam, H.A.; Allam, A.A. Development of Illuminant Glow-in-the-Dark Cotton Fabric Coated by Luminescent Composite with Antimicrobial Activity and Ultraviolet Protection. *J. Fluoresc.* **2019**, *29*, 703–710. [CrossRef] [PubMed]

52. Pisitsak, P.; Hutakamol, J.; Jeenapak, S.; Wanmanee, P.; Nuammaiphum, J.; Thongcharoen, R. Natural dyeing of cotton with xylocarpus granatum bark extract: Dyeing, fastness, and ultraviolet protection properties. *Fibers Polym.* **2016**, *17*, 560–568. [CrossRef]

53. Khattab, T.A.; Abou-Yousef, H.; Kamel, S. Photoluminescent spray-coated paper sheet: Write-in-the-dark. *Carbohydr. Polym.* **2018**, *200*, 154–161. [CrossRef] [PubMed]

54. Pantzas, K.; Patriarche, G.; Troadec, D.; Gautier, S.; Moudakir, T.; Suresh, S.; Largeau, L.; Mauguin, O.; Voss, P.L.; Ougazzaden, A. Nanometer-scale, quantitative composition mappings of InGaN layers from a combination of scanning transmission electron microscopy and energy dispersive X-ray spectroscopy. *Nanotechnology* **2012**, *23*, 455707. [CrossRef]

55. Alghool, S.; El-Halim, H.F.A.; Mostafa, A.M. An eco-friendly synthesis of V 2 O 5 nanoparticles and their catalytic activity for the degradation of 4-nitrophrnol. *J. Inorg. Organomet. Polym. Mater.* **2019**, *29*, 1324–1330. [CrossRef]

56. Eisa, W.H.; Zayed, M.F.; Anis, B.; Abbas, L.M.; Ali, S.S.; Mostafa, A.M. Clean production of powdery silver nanoparticles using *Zingiber officinale*: The structural and catalytic properties. *J. Clean. Prod.* **2019**, *241*, 118398. [CrossRef]